Journal of Neuroscience Methods xxx (2010) xxx–xxx

Contents lists available at ScienceDirect

Journal of Neuroscience Methods

journal homepage: www.elsevier.com/locate/jneumeth

Evaluating the impact of the deep brain stimulation induced electric field on subthalamic neurons: A computational modelling study

Nada Yousif[a,*], Nuri Purswani[b], Richard Bayford[c], Dipankar Nandi[a,d], Peter Bain[a,d], Xuguang Liu[a,d,*]

[a] Department of Clinical Neuroscience, Imperial College London, London, W6 8RP, UK
[b] Department of Bioengineering, Imperial College London, London, SW7 2AZ, UK
[c] The Bio-modelling/Bio-informatics Group, Middlesex University, London, NW4 4BT, UK
[d] The Movement Disorders and Neurostimulation Unit, Charing Cross Hospital, London, W6 8RF, UK

ARTICLE INFO

Article history:
Received 8 October 2009
Received in revised form 19 January 2010
Accepted 21 January 2010

Keywords:
Deep brain stimulation
Multi-compartment models
Subthalamic nucleus
Finite element method
Axon models

ABSTRACT

Deep brain stimulation (DBS) is an effective surgical treatment used to alleviate the symptoms of neurological disorders, most commonly movement disorders. However, the mechanism of how the applied stimulus pulses interact with the surrounding neuronal elements is not yet clearly understood, slowing progress and development of this promising therapeutic technology. To extend previous approaches of using isolated, myelinated axon models used to estimate the effect of DBS, we propose that taking into account entire neurons will reveal stimulation induced effects overlooked by previous studies. We compared the DBS induced volume of tissue activated (VTA) using arrays of whole cell models of subthalamic nucleus (STN) excitatory neurons consisting of a cell body and an anatomically accurate dendritic tree, to the common models of axon arrays. Our results demonstrate that STN neurons have a higher excitation threshold than axons, as stimulus amplitudes 10 times as large elicit a VTA range a fifth of the distance from the electrode surface. However, the STN neurons do show a change in background firing rate in response to stimulation, even when they are classified as sub-threshold by the VTA definition. Furthermore the whole neuron models are sensitive to regions of high current density, as the distribution of firing is centred on the electrode contact edges These results demonstrate the importance of accurate neuron models for fully appreciating the spatial effects of DBS on the immediate surrounding brain volume within small distances of the electrode, which are overlooked by previous models of isolated axons and individual neurons.

1. Introduction

Computational models have proven to be extremely useful for visualizing and estimating the effects of extracellular stimulation of the human brain, as induced by therapeutic deep brain stimulation (DBS) (McIntyre and Grill, 2001; McIntyre et al., 2004a,b; Hemm et al., 2005; Wei and Grill, 2005; Butson and McIntyre, 2005; Elwassif et al., 2006; Sotiropoulos and Steinmetz, 2007; Yousif et al., 2007; Yousif and Liu, 2007a; Yousif and Liu, 2007b;Yousif et al., 2008a; Yousif et al., 2008b; Vasques et al., 2009). DBS is a surgical treatment used to combat the symptoms of neurological disorders, most commonly movement disorders such as Parkinson's disease, tremor and dystonia and increasingly for psychological disorders (Benabid et al., 1994; Nuttin et al., 2003; Vidailhet et al., 2005; Mayberg et al., 2005; Deuschl et al., 2006; Kupsch et al., 2006). It involves the implantation of quadripolar electrodes into the human brain, through which a high frequency train of constant voltage or constant current square pulses is used to stimulate the surrounding neural tissue. The success of the treatment is marred only by the lack of understanding of how the stimulus interacts with surrounding neuronal activity to induce the observed clinical improvement (Lozano et al., 2002; Benabid, 2007; Kringelbach et al., 2007), particularly as the treatment evolved from empirical investigations in the operating theatre. Restrictions on experimental work make investigations of the mechanisms extremely difficult. Furthermore, direct visualization of the induced current *in vivo* is at present impossible, due to safety issues of magnetic resonance imaging during stimulation, as well as the limitation of stimulus artefact on simultaneous electroencephalography, local field potential recordings (Rossi et al., 2007) and radiological imaging. Therefore, the present day use of DBS lacks a theoretical framework and remains based on trial and error for determining electrode location, electrode montage and parameter settings, which is sub-optimal. Furthermore, future development of DBS for new disorders and targets is slowed by the necessity of taking this empirical approach. These constraints

* Corresponding authors. 10L24 Charing Cross Hospital, Imperial College, London, W6 8RF, UK. Tel.: +44 207 88427042.
E-mail addresses: n.yousif@imperial.ac.uk (N. Yousif), x.liu@imperial.ac.uk (X. Liu).

0165-0270/$ – see front matter © 2010 Elsevier B.V. All rights reserved.
doi:10.1016/j.jneumeth.2010.01.026

further inhibit our ability to understand how the stimulus interacts with the neurons and the neuronal networks involved in the pathology.

Hypotheses for the mechanisms underlying the effects of DBS of the subthalamic nucleus (STN), the most common target for Parkinson's disease, range from the activation of fibres of passage leading to over excitation of downstream structures and in turn inhibiting the thalamus and cortex, to the disruption of network wide pathological synchronization allowing the patient to emerge from disabling symptoms such as tremor, rigidity and a variety of akinesias (Lozano et al., 2002; Benabid et al., 2002; Kringelbach et al., 2007). In recent years, two modelling approaches have proven particularly useful and contributed to our ability to probe such hypotheses. The first focuses on models of synchronized activity in the basal ganglia, or the basal ganglia thalamocortical network (Tass, 2003; Rubin and Terman, 2004; Hauptmann et al., 2005; Leblois et al., 2006; Hauptmann et al., 2007; Shils et al., 2008). While this is an interesting approach to investigating ideas of desynchronization of pathological synchrony, most models do not take into account the geometry of the brain tissue and the spatial spread of current in the brain volume surrounding a DBS electrode. The second uses a finite element model to visualize the electric field distribution over a geometry of interest (McIntyre and Grill, 2001; McIntyre et al., 2004a,b; Hemm et al., 2005; Wei and Grill, 2005; Gimsa et al., 2006; Elwassif et al., 2006; Astrom et al., 2006; Yousif et al., 2007; Yousif and Liu, 2007a; Yousif and Liu, 2007b; Yousif et al., 2008a; Yousif et al., 2008b; Vasques et al., 2009) and couples the results to cable models of single neurons (Miocinovic et al., 2006) or arrays of axons (Butson and McIntyre, 2005; Miocinovic et al., 2006; Butson and McIntyre, 2006; Sotiropoulos and Steinmetz, 2007; Butson et al., 2007; Butson and McIntyre, 2008) for quantifying the volume of tissue activated (VTA) in the surrounding brain volume. Single neuron models demonstrate how the field affects a single point in the brain volume, while the VTA approach classifies activated points as those where the axon models fire in a 1:1 ratio with the stimulus train pulses and plots this spatially. However, when an electrode is implanted into a grey matter structure such as the STN, the surrounding brain volume contains a local network of excitatory neurons in addition to passing fibres. One recent study used a combined approach to analytically determine the spread of current in space and applied this to a large scale basal ganglia network model which accounts for individual cell dynamics (Arle et al., 2008; Shils et al., 2008). This study clearly demonstrated the importance of considering all levels of description from local current spread to network dynamics for understanding the mechanisms of DBS on pathological neural activity.

The anatomy and physiology of the STN has been studied in detail in the past in a variety of species and in health and disease (Kita et al., 1983; Afsharpour, 1985; Wichmann et al., 1994; Bevan and Wilson, 1999). In vitro and in vivo subthalamic projection neurons fire spontaneously in the absence of current injection and synaptic input, discharging continuously and repetitively at low frequencies (Bevan and Wilson, 1999;Beurrier et al., 1999). During movement, they have been found to respond to synaptic input and fired repetitively at much higher frequencies (Wichmann et al., 1994;Beurrier et al., 1999). Based on this wealth of information Gillies and Willshaw (2006) produced and reported a detailed model of STN excitatory neurons which form the basis of the signalling in the STN. Previous work has used this model to look at the effects of applying an electrical field to a single cell placed in the different locations within the brain volume surrounding a DBS electrode (Miocinovic et al., 2006). Such work revealed some of the principles of how an applied electrical field affects individual neurons, however it neglected the spatial effect of the induced electric field on influencing a population of neurons, which can be revealed by using model arrays and plotting a VTA.

In the present study, we hypothesized that the VTA will be insufficiently represented by arrays of myelinated axons to represent the surrounding brain volume, as the morphology and physiology of the nearby neuronal elements may be over-simplified. Therefore the objective of the present study is to quantify the difference in VTA estimations using different neuronal elements in the STN region, selectively taking into account the local neuronal network and the passing axons. Hence, we estimated the VTA using arrays of neurons representative of the STN and directly compared this with VTA plots using arrays of myelinated axon models. We found that the VTA alone was inadequate for visualizing the effects of stimulation on neurons, as subtle changes in the firing rate were overlooked. Instead in the present study we propose an additional measure we have called the volume of tissue stimulated (VTS), which defines a stimulated point in the tissue as one where a neuron's firing rate is changed relative to the spontaneous firing rate.

2. Materials and methods

The methodology used here involves simulating DBS via a finite element model which represent the geometry of the problem, and using the obtained potential distribution to stimulate a range of neuronal models. Each step is explained in turn in the following sections.

2.1. The finite element approach

The generic depth electrode-brain interface (EBI) has been previously defined based on physiological recordings and post-mortem examination of the stimulation site in patients (Yousif et al., 2007;Yousif and Liu, 2007b;Yousif et al., 2008a;Yousif et al., 2008b). In order to focus on the novel method of VTA estimation, the EBI model was simplified in this study, by neglecting the peri-electrode space. Therefore the geometry consists of: (i) the implanted DBS electrode(s) based on the manufacturer's description of the quadripolar electrode (model 3389, Medtronic, MN, USA) and (ii) the surrounding brain tissue. The modelling package COMSOL Multiphysics 3.3 (COMSOL AB, Stockholm, Sweden) was used to create a two-dimensional axi-symmetric geometrical representation of the EBI, with the precise electrode dimensions and the surrounding tissue was modelled as a rectangle with a width of 100 mm. The defined geometry is meshed using the default Delaunay triangulation method in COMSOL. The adaptive mesh option was then used in order to refine the mesh at the regions within the geometry where the potential changes most over space. This improves the accuracy of the solution in such regions, which are in fact in the vicinity of active electrode contacts.

The potential distribution induced by stimulation was calculated by solving the Laplace equation:

$$\nabla.\sigma\nabla V = 0$$

where V is the potential (measured in V), σ is the constant conductivity (measured in S/m), ∇ is the gradient of the potential, such that $\nabla V = (\frac{\partial V}{\partial x}, \frac{\partial V}{\partial y}, \frac{\partial V}{\partial z})$ thus resulting in a vector field, and $\nabla.$ is the divergence of that vector field, representing the sum of the partial derivatives in each spatial coordinate, such that for a vector F, $\nabla.F = \frac{\partial F_x}{\partial x} + \frac{\partial F_y}{\partial y} + \frac{\partial F_z}{\partial z}$. The mean conductivity values of the brain tissue were defined based on previous biological studies with gray matter 0.2 S/m. Active contacts were set to the desired stimulating potential in volts, and the outer boundary was constrained to 0 V via Dirichlet boundary conditions. For monopolar stimulation this boundary condition represents the stimulator case which is far from the electrode contact being grounded, as in clinical practice. The non-active contacts and insulating parts of the implanted electrode were bound using Neumann conditions, constraining the

Please cite this article in press as: Yousif N, et al. Evaluating the impact of the deep brain stimulation induced electric field on subthalamic neurons: A computational modelling study. J Neurosci Methods (2010), doi:10.1016/j.jneumeth.2010.01.026

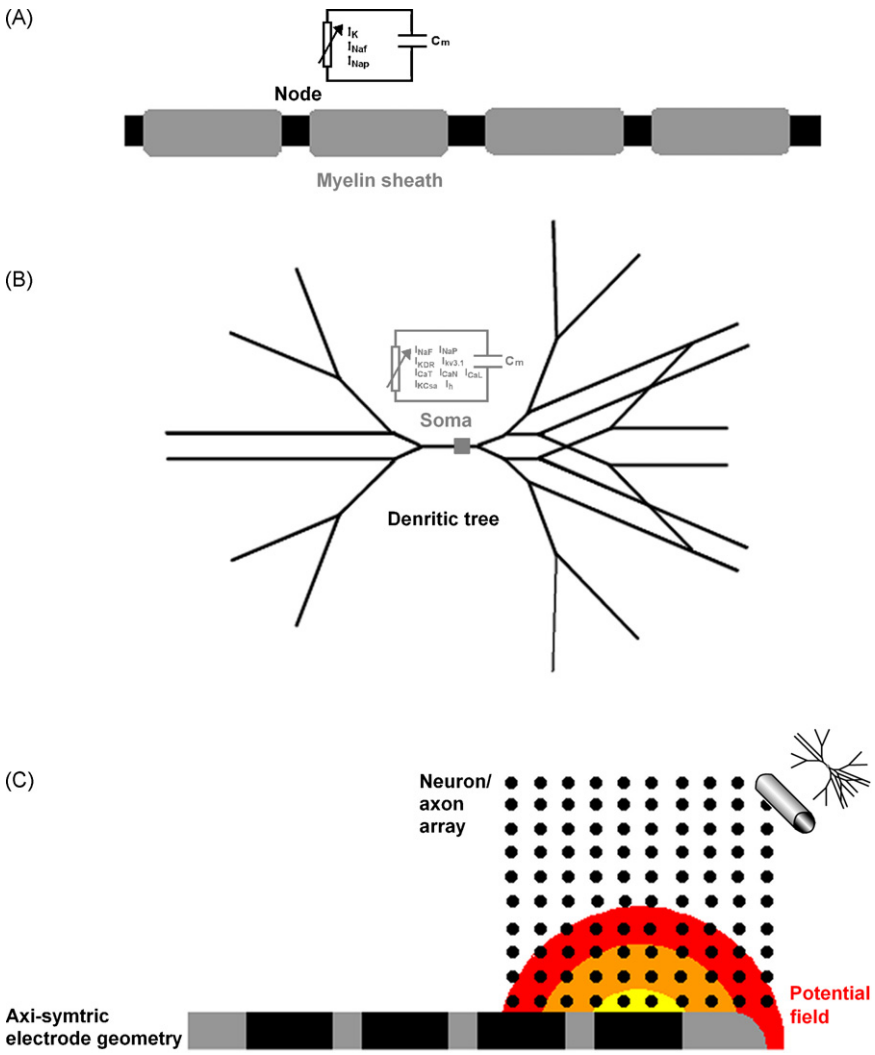

Fig. 1. The figure shows the schematic geometry of the models used to estimate the effect of deep brain stimulation on surrounding tissue. (A) A section of McIntyre's previously presented axon model is shown here to demonstrate the morphology of a myelinated neuronal fibre and the membrane dynamics of the nodal compartment. The node contains a potassium current (I_K) and two sodium currents (I_{Naf} and I_{Nap}) which are each represented by a voltage dependent resistor. Each ion channel is therefore in parallel with one another and the membrane capacitance C_m. (B) Gillies and Willshaw's STN neuron model has a cell body and full dendritic tree consisting of a single tree repeated three times. The somatic membrane dynamics contain numerous ion channels (I_{Naf}, I_{Nap}, I_{KDR}, $I_{kv3.1}$, I_{CaT}, I_{CaN}, I_{CaL}, I_{KCsa} and I_h), in parallel with the membrane capacitance. (C) These models are used to estimate the effect of an extracellular electric field on the firing properties of surrounding neurons. The electric field is estimated in an axi-symmetric finite element model of the DBS electrode, which yields the potential distribution in space. The potential values are convolved by a square pulse representing the DBS stimulus and applied to the compartmental models, which are arranged with the central node (axons) or soma (neurons) in the plane of the electrode, with their long axis perpendicular to the axis of the electrode and at the points marked by the black dots in the figure.

derivative of the electric potential through these boundaries to be zero, i.e. there is no current flow through these boundaries.

2.2. Axon models

In order to compare the stimulation induced effects in surrounding neurons to the established approach, we first used compartmental models of myelinated unconnected axons (Fig. 1A) using cable theory. The model we used is that of McIntyre et al. (Butson et al., 2006), and is briefly described here. Double-cable models represent both the myelin sheath and the axolemma, with explicit representation of the nodes of Ranvier, paranodal and internodal segments. Implementing the models in NEURON v6.2, we used the 5.7 μm diameter axons, which contain a fast sodium conductance, a persistent sodium conductance, and a slow potassium conductance at the nodes. We modelled 100 such axons in a 10×10 configuration, which were stimulated extracellularly using the induced electric potential estimated by the FEM model, convolved with a time dependent square wave for 100 ms.

2.3. STN neuron models

The STN projection neuron model (Fig. 1B) we utilized was previously published by Gillies and Willshaw (2006), and is based on the complex dynamics and morphology of rat STN neurons. The STN morphology consists of a soma and three dendritic trees, as previously reported (Kita et al., 1983;Afsharpour, 1985). The dendrites are passive cables and do not contain any active conductances. The somatic physiology is based on fast and persistent sodium currents (NaF and NaP) as well as delayed and fast rectifier potassium currents (KDR and kv3.1). In addition, low voltage activated (CaT) and high voltage activated (HVA) calcium currents (CaN and CaL) were included as well as calcium controlled K+ currents (KCsa) and a hyperpolarization activated cation channel (Ih). These channels combine to generate observed firing patterns at rest. The NaP current is important in controlling both the frequency and amplitude of the slow ramp depolarization before the action potential. The Kv31 channel played a role in reducing the width of the action potential to match STN neurons as closely as possible (Bevan and

Please cite this article in press as: Yousif N, et al. Evaluating the impact of the deep brain stimulation induced electric field on subthalamic neurons: A computational modelling study. J Neurosci Methods (2010), doi:10.1016/j.jneumeth.2010.01.026

Wilson, 1999;Gillies and Willshaw, 2006). KCsa currents and HVA calcium currents are responsible for the emergence of the spontaneous firing properties, intrinsic to STN neurons. Blockade of KCsa currents can result in loss of rhythmicity of firing, and removal of the CaL conductance completely abolishes spontaneous activity of STN neurons. CaT currents were not found proximally in the soma, but were included in the primary dendrites. Calcium currents also control other interesting properties of STN neurons such as rhythmic bursting and post-hyperpolarizing rebound responses. The original model had two different in vitro environments which allowed the cells to display slightly different dynamics. We ran the simulations in both settings and compared the resulting VTA plots. We chose to show the less conservative VTA estimates, in order to demonstrate the minimal difference in the VTA plots obtained with each type of model.

2.4. Definitions of VTA and the new VTS

For consistency with previous studies, we define the VTA in the following way: For both the axons and the neurons, 100 axons/cells were placed in a 10×10 array adjacent to the electrode and orientated with their long axis perpendicular to the electrode shaft (Fig. 1C). The distance between adjacent axon and neuron models was 0.5 mm, which was chosen in order to allow direct comparison with previous methods of quantifying the VTA. Note that simulations were also run with neurons separated by 0.1 mm, but we found that it did not change our results. For each VTA, the potential value was obtained from the FEM model at the coordinates of the centre of each compartment of the multi-compartment model. The FEM results of potential were applied as an extracellular voltage to every compartment of each model after convolution with a DBS pulse train constructed in MATLAB. Pulse trains were defined as monophasic or biphasic and by the amplitude (of the cathodic pulse), frequency and pulse width.

To be consistent with previous studies presenting the VTA, the location of axons/cells which fire at the stimulating frequency is then taken as an activated point in the neural tissue. However, the results from our whole neuron models showed that the VTA neglects subtle stimulation–induced changes in spontaneous firing rate, if the firing rate remains less than the stimulus frequency. Therefore, we introduced the VTS, volume of tissue stimulated. We define a neuron to be stimulated by the DBS pulse train if its spontaneous firing rate changes as a result of stimulation. Hence, we first determined that the number of spontaneously fired action potentials in the 100 ms simulation time period was three. We then plotted the number of action potentials fired during DBS stimulation in a spatial map, as for the VTA. This VTS plot therefore shows both the number of action potentials fired at each location and the region where firing rate changed as a result of stimulation.

3. Results

3.1. The neuronal "VTA"

The neurons displayed intriguing patterns of activity (Fig. 2). The first thing to note is that a −1 V stimulation amplitude did not elicit responses for the neuron models (Fig. 2C), but a much higher amplitude (−10 V) was required. Second, fewer neurons fired in a 1:1 ratio than axons and only two neurons immediately adjacent to the electrode contact fired at the stimulation parameters of −10 V, 90 us, 130 Hz (Fig. 2A). Third, at low levels of activation, only neurons located at the upper and lower edges of the electrode contact, the regions of highest current density, were defined as activated. Finally, when the pulse width is increased to 450 μs (Fig. 2B), and when the stimulus frequency is decreased to 50 Hz (Fig. 2D) the VTA increases so that the neurons within 1 mm of the electrode and at the contact edges fire action potentials.

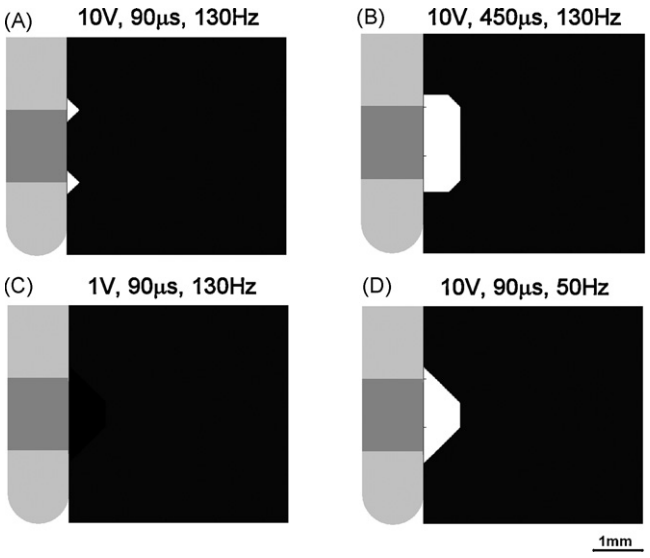

Fig. 2. The VTA plots obtained using the array of STN neurons show the region surrounding the activated DBS electrode contact (in dark grey on left) where axons are activated (white region), or not affected by the stimulus (black region). The plots show that the STN array is much less excitable than the myelinated axons and higher amplitude stimuli were used. (A) −10 V, 90 μs, 130 Hz stimulation activated a single neuron in the surrounding tissue, which was located at the contact's upper edge. (B) When the stimulus pulse width was increased to 450 μs, the range of activation increased to 1 mm away from the electrode surface but remained localized around the contact edges. (C) Stimulating with a 1 V stimulus lead to no neurons firing at the stimulus frequency, therefore none are defined as activated. (D) A change in frequency to 50 Hz stimulated more neurons in a strickingly similar pattern to the longer pulse width stimulus.

3.2. The axonal "VTA"

The axonal VTA plots (Fig. 3) were very similar to those previously reported. In response to a stimulus of amplitude 1 V, all axons

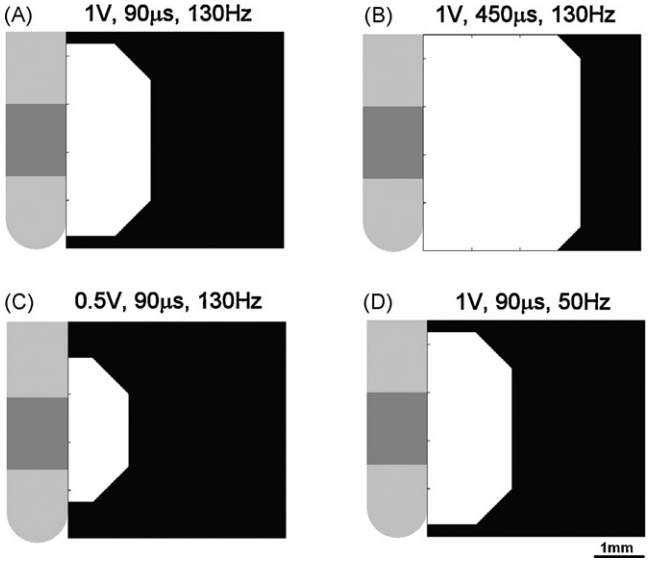

Fig. 3. The axonal VTA plots show greater activation in the surrounding tissue. (A) −1 V, 90 μs, 130 Hz stimulation activates axons up to 2.5 mm away from the electrode surface and in a spatial pattern which is symmetric about the activated. (B) This distance increases (4.5 mm) with increasing pulse width, (C) decreases with decreasing amplitude (2 mm) and (D) does not change with changes to the stimulus frequency.

Please cite this article in press as: Yousif N, et al. Evaluating the impact of the deep brain stimulation induced electric field on subthalamic neurons: A computational modelling study. J Neurosci Methods (2010), doi:10.1016/j.jneumeth.2010.01.026

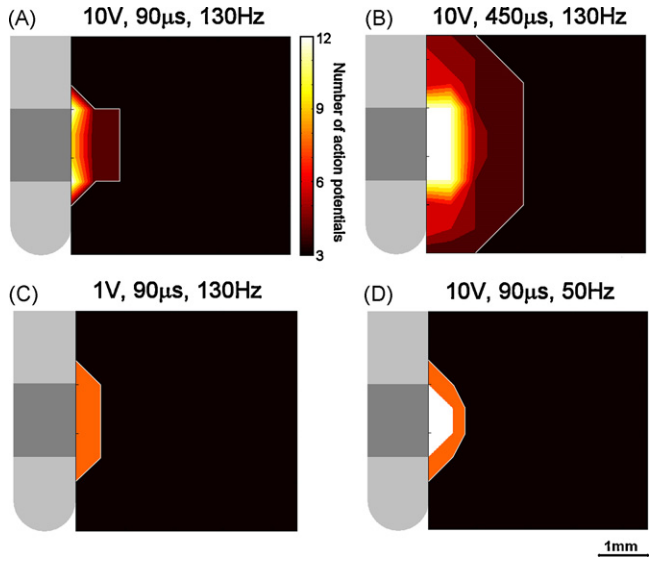

Fig. 4. The STN neuron models are not always induced to fire at the stimulus frequency and therefore do not qualify as "activated" in the VTA definition. However, stimulation does change neuronal rest firing rate of 3 action potentials in the 100 ms simulation period The plots show the number of action potentials for the surrounding neurons (colour bar) and the VTS (white line), defined as the region where neurons' firing rate changes as a result of stimulation. While neurons may not be classified as "activated", their firing rate may still be modulated by stimulation and this may underlie the changes in symptoms. (For interpretation of the references to colour in this figure legend, the reader is referred to the web version of the article).

which were located within 2 mm of the electrode were activated such that they fired an action potential for each pulse of the stimulus train (Fig. 3A). Decreasing the amplitude of stimulation to 0.5 V (Fig. 3C), decreased this distance to less than 1.5 mm, and increasing the pulse width to 450 μs stimulated all axons within 3.5 mm (Fig. 3B). As expected, changing the frequency had no effect on the axon firing pattern (Fig. 3D).

3.3. Comparison of the neuronal "VTA" with the axonal "VTA"

Specifically, the neuronal VTAs are smaller than the axonal VTA plots, even with much greater stimulation amplitudes. When the same amplitude stimulus is used, the axons predict stimulation which reaches 2 mm away, and the neuronal VTA predicts that no activation takes place (Fig. 2C and Fig. 3A). Both neurons and axons show an increase in the activation range with increasing pulse width (Figs. 2B and 4B), and these changes are on the same order of magnitude in both neuronal (100% increase) and axonal (75% increase) plots. Similarly, both models show a decrease in the VTA with reduced stimulus amplitude (Figs. 2C and 3C). Surprisingly, the neuronal VTA increased with a decrease in frequency in the same way as with changing pulse width (Fig. 2D), while the axonal VTA did not change at all (Fig. 3D). Finally, the neuronal VTA plots show more activation at the contact edges at lower activation levels, while the axonal VTA was consistently symmetric about the centre of the activated contact.

3.4. The volume tissue stimulated (VTS)

The VTS plots the region containing neurons affected by the electric field, defined by a stimulus-induced change in spontaneous firing rate. Such neurons are not necessarily "fully activated" as defined in the typical VTA sense. Fig. 4 shows the number of action potentials that were fired in each simulation of the neuron model array and the VTS region highlighted in white. These plots shows that the spontaneous firing rate of 3 action potentials in the 100 ms window was altered due to stimulation even when the VTA plots showed that those neurons were not "fully activated" (Fig. 2). For example, with a −10 V, 90 μs, 130 Hz stimulus only two neurons were activated (Fig. 2A) but the VTS plot (Fig. 4A) reveals that neurons up to 1 mm away were affected by stimulation as their spontaneous firing rates were altered. Furthermore, the VTA demonstrates that no neurons were stimulated with a −1 V amplitude stimulus (Fig. 2C), while the VTS shows that neurons adjacent to the contact edge fired one action potential more than at rest (Fig. 4C). Finally, while the VTA plots for −10 V, 450 μs, 130 Hz (Fig. 2B) and −10 V, 90 μs, 50 Hz (Fig. 2D) stimulation show a similar pattern of activation, the VTS plots demonstrate that very different firing rates are induced by these two stimulus trains (Fig. 4B and D).

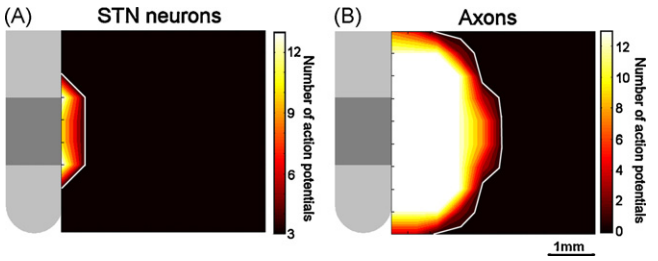

Fig. 5. The VTS plots are repeated with a 130 Hz stimulation train and biphasic pulses. In the neuronal case (A), the cathodal phase was defined as before −10 V and 90 μs wide, and the second anodal phase was defined to have an amplitude of 1 V and a pulse width of 900 μs. In the axonal case (B), the cathodal amplitude was −1 V and pulse width 90 μs and the anodal phase had amplitude of 0.1 V and a 900 μs pulse width. The neuronal VTS is reduced compared to the VTS in the monophasic case (Fig. 4A).

3.5. Biphasic pulses

In practice the DBS pulse train consists of biphasic pulses comprised of an initial cathodal phase (defined by the user selected amplitude and pulse width) and an anodal phase to balance the charge injected, which can be modelled with a smaller amplitude and a longer pulse width. We looked at the axonal and neuronal VTAs induced by such biphasic pulses and found that the VTA remained unchanged (data not shown). However, the VTS in this case did change. Fig. 5 shows the neuronal and the axonal VTS in response to a biphasic train of pulses at 130 Hz, 90 μs and −10 V (neurons) or −1 V (axons). These plots demonstrate that although the VTA was unchanged, the VTS is slightly reduced with biphasic stimulation compared to monophasic (compare Fig. 5A and Fig. 4A).

4. Discussion

In the present study, we investigated the impact of the DBS induced electric field on subthalamic neurons by visualizing and quantifying the VTA using an array of whole neuron models, and comparing our results to results obtained using previously reported arrays of myelinated axon models. Our main findings are: (1) STN neurons are much less excitable than axons, such that to induce "activation" according to the VTA definition using the neuron models requires a stimulation intensity 10 times as high as that required by the axon models. Furthermore, with a −10 V stimulus the distance activated of the former is a fifth of the distance activated with a −1 V stimulus using the latter. (2) Interestingly, however, the STN neurons do show a change in background firing rate in response to stimulation at low intensity, as measured by VTS, even when the firing rate is below threshold for the VTA plots (i.e. less than the stimulus frequency); (3) the whole neuron model estimations show that the activated neurons are primarily concentrated in the regions of high current density at the contact edges; and (4) the

Please cite this article in press as: Yousif N, et al. Evaluating the impact of the deep brain stimulation induced electric field on subthalamic neurons: A computational modelling study. J Neurosci Methods (2010), doi:10.1016/j.jneumeth.2010.01.026

whole neuron VTA plots change with changing stimulus frequency, which is not the case for the axon models.

FEM models solving the Laplace equation have proven extremely useful for visualizing the DBS induced electric field. However, such models do not demonstrate how this field will in turn affect the neurons in the surrounding tissue. Different methods of interpreting the electric field distribution therefore have been used in the past. A straightforward analysis involves assessing the potential distribution directly, such as via the isopotential lines over space (Hemm et al., 2005; Astrom et al., 2006; Yousif et al., 2008a; Yousif et al., 2008b; Vasques et al., 2009). This lacks a direct link to neuronal dynamics. The seminal work of Frank Rattay demonstrated that neuronal membranes are induced to fire action potentials at regions of high spatial difference of the electric field (Rattay, 1989). This concept of the activation function, which is calculated as the second spatial derivative of the potential has also been extensively used, but is not directly linked to the morphology of the neural elements. The activation function is derived from an equivalent circuit model of an axon which can be used for both myelinated and unmyelinated fibers. Rattay showed that when compartmentalizing an axon in this way, the stimulation induced change to the membrane potential is determined by the second spatial derivative of the imposed extracellular potential. The activation function is therefore based on a similar compartmental modelling approach as used in the present study and in previous axonal VTA studies, but gives more information than VTA plots as it accounts for polarization of nerve membranes, not only showing whether axons fire at the stimulation frequency, and, estimating the activation of neural tissue by coupling the results from a FEM model to compartmental cable models of single neurons (McIntyre et al., 2004a,b; Miocinovic et al., 2006; Johnson and McIntyre, 2008) or portions of neurons (most commonly axons) has been used and compared to the activation function (McIntyre et al., 2004a,b). This approach can be considered as the most detailed, but as we have shown here is highly dependent on the compartmental model used.

Previous models assessing the effects of deep brain stimulation on the neuronal activity in the surrounding brain region have predominantly used isolated, myelinated axon models (McIntyre et al., 2004a,b; Butson and McIntyre, 2005; Butson and McIntyre, 2006; Sotiropoulos and Steinmetz, 2007; Yousif and Liu, 2009) to assess the volume of tissue activated, based on the assumption that these fibres are the most excitable neuronal structure in the brain (Ranck, 1975). However, such work has simplified the composition of the surrounding brain volume. When neuron models have been used to investigate stimulation induced effects, such work has focussed on single neuron models (McIntyre et al., 2004a,b; Miocinovic et al., 2006; Johnson and McIntyre, 2008) and therefore has not accounted for the effect of the spatial structure of the field on the stimulation induces effects. One notable exception is the work of Arle and Shils (Arle et al., 2008; Shils et al., 2008), which was based on a multi-level description of the effects of DBS, including an analytical solution for the spatial electric field and an ionic description of the surrounding neurons organized within a network model of the human basal ganglia. This work demonstrated the importance of considering all of these elements in understanding DBS and overcoming the shortcomings of previous studies based only on the isolated axons, and gave us the motivation to carry out the present study of estimating the VTA with an array of neurons and comparing the results to the axonal VTA.

The models used here were based on a previously presented model (Gillies and Willshaw, 2006) of excitatory subthalamic neurons, which were built to mimic the anatomy and physiology of these cells. In particular these cells have an extended dendritic tree, fire spontaneously at a frequency of 10–30 Hz (Kita et al., 1983; Afsharpour, 1985; Wichmann et al., 1994; Bevan and Wilson, 1999; Beurrier et al., 1999), and have been used previously in single neuron models to estimate DBS induced effects (Miocinovic et al., 2006). It ought to be noted that these models are largely based on animal studies of the STN and therefore may not translate directly to the human basal ganglia. However, in line with the DBS modelling literature thus far, we believe that these models are suitable for estimating the relative effects of different parameter settings and configurations if not to reveal the absolute effect of DBS on a case to case basis. We adapted this whole cell model to estimate the effects of stimulation pulses on an anatomically and physiologically plausible neuron population. We modelled the electric field in a two-dimensional axi-symmetric FEM model and the resulting potential distribution was used as the extracellular stimulus for our array of STN neurons. The VTAs obtained from these whole neuron arrays were then compared with an array of myelinated axons. We found that the neurons were much less excitable, and the stimulus amplitude had to be increased ten-fold to observe significant VTA plots. Even with such a strong stimulus (10 V, 90 μs and 130 Hz) only a single neuron adjacent to electrode contact edge fired at this condition. In contrast, the axon models fire robustly to a stimulus with an amplitude as low as 1 V up to a distance of 2.5 mm from the electrode surface, which is consistent with previous reports (McIntyre et al., 2004a,b; Butson and McIntyre, 2005; Butson and McIntyre, 2006; Butson et al., 2006; Sotiropoulos and Steinmetz, 2007).

As with the axon models, an increase in pulse width lead to more neurons being activated. However, the spatial layout of the activated neurons was unpredicted. Surprisingly, the activated neurons were those around the edges of the electrode contact, which is consistent with the regions of high current density. This effect has not been previously demonstrated with axon models as in that case, the models are not sensitive enough to pick up this effect. Even at very low stimulus amplitudes we found that the axon models always predict a VTA which is symmetric about the centre of the activated contact (data not shown). However, this "edge effect" has been shown in previous modelling studies of the DBS induced electric field (Wei and Grill, 2005) and our results show that it may lead to regions of neuronal activation concentrated at the edges of the electrode contacts. Given that the DBS electrode contacts are 1.5 mm long and that changes in clinical outcome are observed with millimetre precision, this may be significant for localizing the therapeutic effect.

The axon models used previously did not show any dependence on the frequency of the stimulation pulse train as expected. Interestingly however, the VTA obtained with the STN neurons was dramatically different when the frequency was reduced. A 10 V, 90 μs, 50 Hz train produced a VTA which was completely different to the 10 V, 90 μs, 130 Hz VTA, but almost identical to the 10 V, 450 μs, 130 Hz VTA. Furthermore, instead of looking only at activation as a measure of inducing responses at the stimulus frequency, we also look at stimulation as any change of firing rate induced by stimulation. This further demonstrated the difference in firing rates induced by different frequency stimulation trains. This change in neuronal response with frequency is a crucial feature of as the improvement in patients' symptoms is only seen with high frequencies in the 100–130 Hz range (Birdno and Grill, 2008) and lower frequencies in fact exacerbate symptoms. We believe that observing a change in stimulation induced effects with changing stimulus frequency is a crucial feature of a DBS model and hence isolated, myelinated axon arrays are inadequate for studying this important question. In addition, stimulation with biphasic pulses showed that changes in spontaneous firing rate is spatially restricted compared to monophasic pulses, as previously shown (e.g. Miller et al., 2001). Hence, it is not only the cathodal portion of the pulse that is important (Merrill et al., 2005), but that both phases contribute to altering neuronal activity.

Please cite this article in press as: Yousif N, et al. Evaluating the impact of the deep brain stimulation induced electric field on subthalamic neurons: A computational modelling study. J Neurosci Methods (2010), doi:10.1016/j.jneumeth.2010.01.026

Despite the interesting results shown here, this model is an initial step towards making accurate estimations of the effect of a stimulation induced field on the firing properties of local neurons. As such there are a number of limitations and assumptions which will need to be refined in ongoing studies of this kind. Note that the model did not display any suppression of firing, though a popular hypothesis is that high frequency stimulation of the STN acts as a functional lesion which silences pathological activity. This maybe due to a lack of accuracy in the modelled neuronal array such as, an insufficient cell density, uni-orientation of the cells relative to the electrode, the lack of inhibitory interneurons or synapses, the fact that the cell parameters were tuned to match in vitro data, or not accounting for waveform shaping due to capacitance. However, at this stage we wanted to keep the model as similar to the standard axonal VTA approach as possible, hence we used a 10×10 array of neurons separated by 0.5 mm and orientated perpendicular to the electrode shaft and considered the effect of stimulation in a 100 ms time window. Similarly, in this specific model we neglected the EBI in order to focus on the novel method of estimating the VTA. This was based on the assumption that the EBI will only alter the field over a short distance and hence it will affect a small number of cells relative to the overall number being considered here. However, we believe that the EBI may prove to be an additional important factor in modulating neuronal firing patterns, particularly when comparing acute and chronic states of the EBI and this will be investigated further in future work. Hence, this study is a first step towards understanding the detailed mechanisms of DBS at the level of neuronal firing and future work will refine the model presented as described here. A main motivation for this work is that we believe that such changes at the local level should translate into network considerations. In order to bridge the gap between electric field models which consider the spatial spread of current and the work from network models, we believe that a detailed understanding of the neurons in the surrounding tissue is required to predict effects more accurately.

5. Concluding remarks

This study shows that the VTA estimated using an array of neuron models reveals more about the underlying mechanisms of extracellular stimulation on the surrounding neuronal population, and is a significant supplement to the previous approach of estimating the effect of stimulation on axonal firing. The combination of neuron models and axon models for estimating the VTA reveals much richer information about DBS induced effects on the surrounding brain volume and may better correlate with stimulus parameter settings and electrode montages, in which the former approach may be viewed as a way to specifically represent the neuropil in the STN, and the latter a way to quantify the stimulus-induced effects on axons. By comparing VTA plots estimated using neuron and axon models, our results have shown that neurons fire much less in response to the stimulus than myelinated axons and hence there is a significant difference in the size and spatial distribution of the VTA in response to the stimulus of the same intensity. We propose that the stimulus-induced full neuron activation, as measured by the VTA, may be not as important functionally as modulation of neuronal firing rate as measured by the VTS. On the other hand, our present results also suggest that neurons have an activation threshold as 10 times high as that of the myelinated axons, while the intensity for effective therapeutic stimulation usually being in the range of a few Volts. This may suggest that the activation of local neurons may not be the main factor for producing clinical outcomes. However, further work will develop the anatomical and physiological complexity of this model and may demonstrate that synaptic connectivity and increased cell densities lead to larger volumes of neurons affected by stimulation.

Acknowledgements

Nada Yousif was supported by a fellowship from the Medical Research Council of the UK (grant Id. 78512).

References

Afsharpour S. Light microscopic analysis of Golgi-impregnated rat subthalamic neurons. J Comp Neurol 1985;236:1–13.
Arle JE, Mei LZ, Shils JL. Modelling parkinsonian circuitry and the DBS electrode. I. Biophysical background and software. Stereotact Funct Neurosurg 2008;86:1–15.
Astrom M, Johansson JD, Hariz MI, Eriksson O, Wardell K. The effect of cystic cavities on deep brain stimulation in the basal ganglia: a simulation-based study. J Neural Eng 2006;3:132–8.
Benabid AL. What the future holds for deep brain stimulation. Expert Rev Med Dev 2007;4:895–903.
Benabid AL, Pollak P, Gross C, Hoffmann D, Benazzouz A, Gao DM, et al. Acute and long-term effects of subthalamic nucleus stimulation in Parkinson's disease. Stereotact Funct Neurosurg 1994;62:76–84.
Benabid AL, Benazzous A, Pollak P. Mechanisms of deep brain stimulation. Mov Disord 2002;17(Suppl 3):S73–4.
Beurrier C, Congar P, Bioulac B, Hammond C. Subthalamic nucleus neurons switch from single-spike activity to burst-firing mode. J Neurosci 1999;19:599–609.
Bevan MD, Wilson CJ. Mechanisms underlying spontaneous oscillation and rhythmic firing in rat subthalamic neurons. J Neurosci 1999;19:7617–28.
Birdno MJ, Grill WM. Mechanisms of deep brain stimulation in movement disorders as revealed by changes in stimulus frequency. Neurotherapeutics 2008;5:14–25.
Butson CR, McIntyre CC. Tissue and electrode capacitance reduce neural activation volumes during deep brain stimulation. Clin Neurophysiol 2005;116:2490–500.
Butson CR, McIntyre CC. Role of electrode design on the volume of tissue activated during deep brain stimulation. J Neural Eng 2006;3:1–8.
Butson CR, McIntyre CC. Current steering to control the volume of tissue activated during deep brain stimulation. Brain Stimulation 2008;1:7–15.
Butson CR, Maks CB, McIntyre CC. Sources and effects of electrode impedance during deep brain stimulation. Clin Neurophysiol 2006;117:447–54.
Butson CR, Cooper SE, Henderson JM, McIntyre CC. Patient-specific analysis of the volume of tissue activated during deep brain stimulation. Neuroimage 2007;34:661–70.
Deuschl G, Schade-Brittinger C, Krack P, Volkmann J, Schafer H, Botzel K, et al. A randomized trial of deep brain stimulation for Parkinson's disease. N Engl J Med 2006;355:896–908.
Elwassif MM, Kong Q, Vazquez M, Bikson M. Bio-heat transfer model of deep brain stimulation induced temperature changes. J Neural Eng 2006;3:306–15.
Gillies A, Willshaw D. Membrane channel interactions underlying rat subthalamic projection neuron rhythmic and bursting activity. J Neurophysiol 2006;95:2352–65.
Gimsa U, Schreiber U, Habel B, Flehr J, van RU, Gimsa J. Matching geometry and stimulation parameters of electrodes for deep brain stimulation experiments—Numerical considerations. J Neurosci Methods 2006;150:212–27.
Hauptmann C, Popovych O, Tass PA. Effectively desynchronizing deep brain stimulation based on a coordinated delayed feedback stimulation via several sites: a computational study. Biol Cybern 2005;93:463–70.
Hauptmann C, Popovych O, Tass PA. Desynchronizing the abnormally synchronized neural activity in the subthalamic nucleus: a modelling study. Expert Rev Med Dev 2007;4:633–50.
Hemm S, Mennessier G, Vayssiere N, Cif L, Coubes P. Co-registration of stereotactic MRI and isofield lines during deep brain stimulation. Brain Res Bull 2005;68:59–61.
Johnson MD, McIntyre CC. Quantifying the neural elements activated and inhibited by globus pallidus deep brain stimulation. J Neurophysiol 2008;100:2549–63.
Kita H, Chang HT, Kitai ST. The morphology of intracellularly labeled rat subthalamic neurons: a light microscopic analysis. J Comp Neurol 1983;215:245–57.
Kringelbach ML, Jenkinson N, Owen SL, Aziz TZ. Translational principles of deep brain stimulation. Nat Rev Neurosci 2007;8:623–35.
Kupsch A, Benecke R, Muller J, Trottenberg T, Schneider GH, Poewe W, et al. Pallidal deep brain stimulation in primary generalized or segmental dystonia. N Engl J Med 2006;355:1978–90.
Leblois A, Boraud T, Meissner W, Bergman H, Hansel D. Competition between feedback loops underlies normal and pathological dynamics in the basal ganglia. J Neurosci 2006;26:3567–83.
Lozano AM, Dostrovsky J, Chen R, Ashby P. Deep brain stimulation for Parkinson's disease: disrupting the disruption. Lancet Neurol 2002;1:225–31.
Mayberg HS, Lozano AM, Voon V, McNeely HE, Seminowicz D, Hamani C, et al. Deep brain stimulation for treatment-resistant depression. Neuron 2005;45:651–60.
McIntyre CC, Grill WM. Finite element analysis of the current density and electric field generated by metal microelectrodes. Ann Biomed Eng 2001;29:227–35.
McIntyre CC, Grill WM, Sherman DL, Thakor NV. Cellular effects of deep brain stimulation: model-based analysis of activation and inhibition. J Neurophysiol 2004a;91:1457–69.

Please cite this article in press as: Yousif N, et al. Evaluating the impact of the deep brain stimulation induced electric field on subthalamic neurons: A computational modelling study. J Neurosci Methods (2010), doi:10.1016/j.jneumeth.2010.01.026

McIntyre CC, Mori S, Sherman DL, Thakor NV, Vitek JL. Electric field and stimulating influence generated by deep brain stimulation of the subthalamic nucleus. Clin Neurophysiol 2004b;115:589–95.
Merrill DR, Bikson M, Jeffreys JGR. Electrical stimulation of excitable tissue: design of efficacious and safe protocols. J Neural Eng 2005;141:171–98.
Miller CA, Robinson BK, Rubinstein JT, Abbas PJ, Runge-Samuelson CL. Auditory nerve responses to monophasic and biphasic electric stimuli. Hear Res 2001;151:79–94.
Miocinovic S, Parent M, Butson CR, Hahn PJ, Russo GS, Vitek JL, et al. Computational analysis of subthalamic nucleus and lenticular fasciculus activation during therapeutic deep brain stimulation. J Neurophysiol 2006;96:1569–80.
Nuttin BJ, Gabriels LA, Cosyns PR, Meyerson BA, Andreewitch S, Sunaert SG, et al. Long-term electrical capsular stimulation in patients with obsessive-compulsive disorder. Neurosurgery 2003;52:1263–72.
Ranck JB. Which elements are excited in electrical stimulation of mammalian central nervous system: a review. Brain Res 1975;98:417–40.
Rattay F. Analysis of models for extracellular fiber stimulation. IEEE Trans Biomed Eng 1989;36:676–82.
Rossi L, Foffani G, Marceglia S, Bracchi F, Barbieri S, Priori A. An electronic device for artefact suppression in human local field potential recordings during deep brain stimulation. J Neural Eng 2007;4:96–106.
Rubin JE, Terman D. High frequency stimulation of the subthalamic nucleus eliminates pathological thalamic rhythmicity in a computational model. J Comput Neurosci 2004;16:211–35.
Shils JL, Mei LZ, Arle JE. Modelling parkinsonian circuitry and the DBS electrode. II. Evaluation of a computer simulation model of the basal ganglia with and without subthalamic nucleus stimulation. Stereotact Funct Neurosurg 2008;86:16–29.
Sotiropoulos SN, Steinmetz PN. Assessing the direct effects of deep brain stimulation using embedded axon models. J Neural Eng 2007;4:107–19.
Tass PA. A model of desynchronizing deep brain stimulation with a demand-controlled coordinated reset of neural subpopulations. Biol Cybern 2003;89:81–8.
Vasques X, Cif L, Hess O, Gavarini S, Mennessier G, Coubes P. Stereotactic model of the electrical distribution within the internal globus pallidus during deep brain stimulation. J Comput Neurosci 2009;26:109–18.
Vidailhet M, Vercueil L, Houeto JL, Krystkowiak P, Benabid AL, Cornu P, et al. Bilateral deep brain stimulation of the globus pallidus in primary generalized dystonia. N Engl J Med 2005;352:459–67.
Wei XF, Grill WM. Current density distributions, field distributions and impedance analysis of segmented deep brain stimulation electrodes. J Neural Eng 2005;2:139–47.
Wichmann T, Bergman H, DeLong MR. The primate subthalamic nucleus. I. Functional properties in intact animals. J Neurophysiol 1994;72:494–506.
Yousif N, Liu X. Investigating the mechanisms of deep brain stimulation: computational modelling approaches–A Commentary. Curr Med Lit Neurol 2007a;23:29–34.
Yousif N, Liu X. Modelling the current distribution across the depth electrode-brain interface in deep brain stimulation. Expert Rev Med Dev 2007b;4:623–31.
Yousif N, Liu X. Investigating the depth electrode-brain interface in deep brain stimulation using finite element models with graded complexity in structure and solution. J Neurosci Methods 2009.
Yousif N, Bayford R, Bain PG, Liu X. The peri-electrode space is a significant element of the electrode-brain interface in deep brain stimulation: a computational study. Brain Res Bull 2007;74:361–8.
Yousif N, Bayford R, Liu X. The influence of reactivity of the electrode-brain interface on the crossing electric current in therapeutic deep brain stimulation. Neuroscience 2008a;156:597–606.
Yousif N, Bayford R, Wang S, Liu X. Quantifying the effects of the electrode-brain interface on the crossing electric currents in deep brain recording and stimulation. Neuroscience 2008b;152:683–91.

Please cite this article in press as: Yousif N, et al. Evaluating the impact of the deep brain stimulation induced electric field on subthalamic neurons: A computational modelling study. J Neurosci Methods (2010), doi:10.1016/j.jneumeth.2010.01.026